Generation of time-bin entangled photon pairs using a quantum-dot cavity system

P. K. Pathak and S. Hughes
Department of Physics, Queen's University, Kingston, ON K7L 3N6, Canada
(Dated: October 11, 2010)

We present a scheme to realize a deterministic solid state source of time-bin entangled photon pairs using cavity-assisted stimulated Raman adiabatic passage (STIRAP) in a single quantum dot. The quantum dot is embedded inside a semiconductor cavity, and the interaction of a coherent superposition of two temporally separated input pulses and the cavity mode leads to a two-photon Raman transition, which produces a time-bin entangled photon pair through the biexciton-exciton cascade. We show that the entanglement of the generated state can be measured using triple coincidence detection, and the degree of entanglement is quantified as the visibility of the interference. We also discuss the effect of pure dephasing on entanglement of the generated photon pair. Pronounced interference visibility values of greater than $1/\sqrt{2}$ are demonstrated in triple coincidence measurement using experimentally achievable parameters, thus demonstrating that the generated photons are suitable for applications with Bell's inequality violation and quantum cryptography.

PACS numbers: 03.65.Ud, 03.67.Mn, 42.50.Dv

arXiv:1010.1713v1 [quant-ph] 8 Oct 2010

I. INTRODUCTION

A source of entangled photon pairs is an essential building block for various quantum information processing protocols[1], such as quantum cryptography[2] and quantum teleportation[3]. Generally, the employed entangled state of photons in these experiments are entangled in both the energy and the polarization degrees of freedom[4]. However, because of unavoidable polarization dispersion in optical fibers, the polarization entangled photons are not suitable for distribution over large distances. In related experiments[5–8], entangled states of photons in energy and time degrees of freedom, using discrete time interval (time-bin) for photon emission, have been demonstrated and the entanglement between these photons has been successfully distributed over distance of 50 km[8]. In these experiments, the time-bin entangled photons were generated through the parametric down convertor (PDC) using the pump as a superposition of two time separated pulses. A PDC is a heralded source of entangled photons where the number of generated photon pairs are probabilistic[9]. At low pump intensity, when the probability of generating more than one photon pair remains small, the efficiency of the source remains very low (less than 20%[7]). For quantum information processing applications, one requires a scalable source which generates precisely a single photon pair on demand[10]. In the last few years, there has been considerable progress for developing *on demand* single photon and entangled photon sources using single quantum dots (QDs)[11–14], where the QDs provide the potential advantages of integrability and scalability in such experiments. In semiconductor QDs, polarization entangled photons have been successfully generated in the biexciton-exciton cascade decay[12–14].

In 2005, Simon and Poizat[15] proposed an on-demand generation of time-bin entangled photons through the biexciton-exciton cascade in idealized QDs, where the bi-exciton state is created by pumping through two pulses interacting at two distinct times. The state of the time-bin entangled photon pair is given by $|\psi\rangle = \sqrt{p_1}|early\rangle_1|early\rangle_2 + e^{i\theta}\sqrt{p_2(1-p_1)}|late\rangle_1|late\rangle_2$, where *early* and *late* are two time bins and p_1 is the probability of generating a photon pair in the early time bin (from the first pulse) and p_2 is probability of generating a photon pair in the late time bin (from the second pulse); the total probability is then $p_1 + p_2 = 1$. For generating maximally entangled state $|\psi\rangle$, one requires $p_1 = p_2 = 1/2$. Therefore, a precisely regulated population transfer between the QD energy levels is essential. Moreover, pure dephasing processes present in semiconductor produce detrimental effects on the entanglement of the generated state. In quantum information protocols, such as entanglement swapping, it is essential that the photons should not have any other correlation except the time-bin entanglement. However, in the biexciton-exciton cascade, emitted photons also have time correlations. These undesirable temporal correlations can be minimized by manipulating emission rates of photons using resonant cavities[15].

In this work, we propose to generate an efficient time-bin entangled photon pair using stimulated Raman adiabatic passage (STIRAP). The coherent excitation in the system of QDs embedded in a semiconductor cavity have been an active area of research[17,18]. We consider the initial QD state is in a metastable state, and there have been several methods for achieving this using electrical control of QD-cavity mode resonce[19,20]. We demonstrate that the STIRAP process then provides an efficient regulated way for population transfer. We also investigate how the cavity enhanced decay rates suppress the detrimental effects of pure dephasing.

Our paper is organized as follows. In Sec. II, we present a formal theory of generation of time-bin entangled photon pair from a single QD coupled to a semiconductor cavity. In Se. III, we investigate the measure of photon entanglement by a triple coincidence detection and also study the effects of dephasing. In section IV, we present our conclusions.

II. GENERATING TIME-BIN ENTANGLED PHOTON PAIRS USING STIRAP

We consider a QD embedded in a semiconductor microcavity, where the energy level diagram of the system is shown in Fig. 1. The dipole transitions from the biexciton state $|u\rangle$ to the exciton state $|y\rangle$, and from the exciton state $|y\rangle$ to the ground state $|g\rangle$, are coupled through a y-polarized single mode of the semiconductor cavity, with coupling constants g_1 and g_2, respectively. Because of the large biexciton binding energy of semiconductor QDs, it is not possible to couple the biexciton and exciton transitions from the same cavity mode, and thus manipulation of the biexciton binding energy becomes essential in these systems[21,22]. Usually the binding energy of the charge-neutral biexciton has a negative value, however by changing the confinement size[23] or by changing the strain[24], it has been found that the biexciton binding energy can be tuned to zero or a positive value. Very recently, manipulation of the binding energy of the biexciton has also been reported by applying lateral electric fields[22]. Moreover, construction of an electrode for applying a lateral electric field in the vicinity of a QD within a photonic crystal cavity has also been reported[19]. Therefore, it is now possible to manipulate the binding energy of biexcitons inside semiconductor cavities. The another advantage of lateral electric fields is that they can be used to create a voltage-tunable metastable exciton state $|m\rangle$.

In III-V QDs, bright netral excitons are formed when an electron from the $s-$shell or the $p-$shell of the valance band is excited to the $s-$shell or $p-$shell of the conduction band, respectively; the transitions from $s-$shell to $p-$shell and vice versa are essentially *symmetrically forbidden*. However, in the presence of an applied lateral voltage, the charge carrier symmetry can be suitably broken broken so that a bright exciton is formed, e.g., from the $s-$shell conduction band to $p-$shell conduction band[22]. Consequently, by applying a lateral voltage larger than the values required to break the symmetry, and then using a π pulse excitation to this state, a symmetrically forbidden exciton can be created which behaves as the metastable state $|m\rangle$, after lowering the applied voltage again. In what follows below, we will assume that this initial state can be created and focus on its evolution after applying STIRAP pulses.

Initially, the QD is prepared in the metastable state $|m\rangle$ and the cavity mode in the vacuum state. An x-polarized pump field with a Rabi frequency $\Omega_p(t)$ is applied between the metastable state $|m\rangle$ and the biexciton state $|u\rangle$. The Hamiltonian of the system, in the rotating frame at the pump frequency (interaction picture), can be written as

$$H = \hbar\Delta_p|m\rangle\langle m| + \hbar\Delta_1|y\rangle\langle y| + \hbar(\Delta_1+\Delta_2)|g\rangle\langle g| + \hbar\left[\Omega_p(t)|u\rangle\langle m| + g_1|u\rangle\langle y|a + g_2|y\rangle\langle g|a + H.c.\right], \quad (1)$$

where Δ_p, and Δ_1 (Δ_2) are the detunings of the pump field, and the cavity mode with the biexciton (exciton) transition frequencies, respectively; $H.c$ refers to Hermitian conjugate. For simulating the dynamics of the system, we perform quantum master equation calculations in the density matrix representation. The evolution of the QD-cavity system is given by

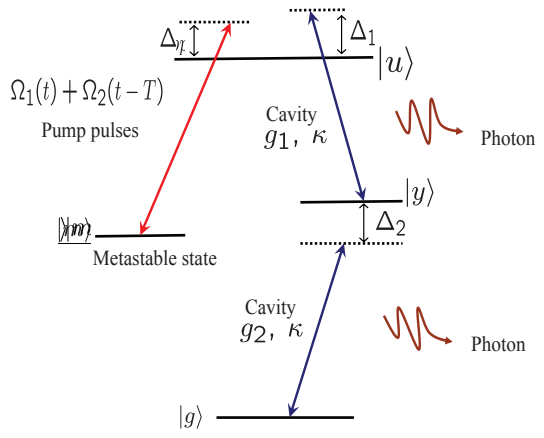

FIG. 1: (Color online) Schematic diagram for time-bin entangled photon generation. The transitions from the biexciton state $|u\rangle$ to the exciton states $|y\rangle$ and $|y\rangle$ to ground state $|g\rangle$ are coupled by a y-polarized cavity mode. The QD is pumped from the metastable state $|m\rangle$ to biexciton state through the superposition of two input pulses.

$$\dot{\rho} = -\frac{i}{\hbar}[H,\rho] - \frac{1}{2}\sum_{\mu}[L_\mu^\dagger L_\mu\rho - 2L_\mu\rho L_\mu^\dagger + \rho L_\mu^\dagger L_\mu], \quad (2)$$

where L_μ are the Lindblad operators, with terms $\sqrt{\gamma_1}|m\rangle\langle u|$, $\sqrt{\gamma_1}|y\rangle\langle u|$, and $\sqrt{\gamma_2}|g\rangle\langle y|$ corresponding to the spontaneous decays, and $\sqrt{2\gamma_d}|u\rangle\langle u|$, $\sqrt{\gamma_d}|m\rangle\langle m|$, and $\sqrt{\gamma_d}|y\rangle\langle y|$, corresponding to pure dephasing of the biexciton and exciton states. The emission of the photons from the cavity mode is given by the Lindblad operator $\sqrt{\kappa}a$, where 2κ is the decay rate of the leaky cavity. We safely neglect the spontaneous decay of the metastable state $|m\rangle$ during the evolution, as the lifetime of the metastable state is, by definition, very large.

We numerically solve the optical Bloch equations using Eq. (2), for density matrix elements $\rho_{ij} = \langle i|\rho|j\rangle$. To simplify the nottaion, we use the definitions $|Y\rangle = |y,1\rangle$, $|G\rangle = |g,1\rangle$, and $|G'\rangle = |g,2\rangle$, where the alpha-numeric notation corresponds to the energy state of QD and the number corresponds to the cavity photon. The complete dynamics of the system is expressed by the following

equations of motion:

$$\dot{\rho}_{mm} = -i\Omega_p^*(t)\rho_{um} + i\Omega_p(t)\rho_{mu} + \gamma_1\rho_{uu}, \quad (3)$$

$$\dot{\rho}_{uu} = i\Omega_p^*(t)\rho_{um} - i\Omega_p(t)\rho_{mu} + ig_1\rho_{uY} - ig_1\rho_{Yu} - 2\gamma_1\rho_{uu}, \quad (4)$$

$$\dot{\rho}_{YY} = -ig_1\rho_{uY} + ig_1\rho_{Yu} - ig_2\sqrt{2}\rho_{G'Y} + ig_2\sqrt{2}\rho_{YG'} - (\kappa+\gamma_2)\rho_{YY}, \quad (5)$$

$$\dot{\rho}_{G'G'} = ig_2\sqrt{2}\rho_{G'Y} - ig_2\sqrt{2}\rho_{YG'} - 2\kappa\rho_{G'G'}, \quad (6)$$

$$\dot{\rho}_{GG} = ig_2(\rho_{Gy}+\rho_{yG}) + 2\kappa\rho_{G'G'} + \gamma_2\rho_{YY} - \kappa\rho_{GG}, \quad (7)$$

$$\dot{\rho}_{yy} = -ig_2(\rho_{Gy}-\rho_{yG}) + \kappa\rho_{YY} + \gamma_1\rho_{uu} - \gamma_2\rho_{yy}, \quad (8)$$

$$\dot{\rho}_{gg} = \kappa\rho_{GG} + \gamma_2\rho_{yy}, \quad (9)$$

$$\dot{\rho}_{um} = -i\Delta_p\rho_{um} - i\Omega_p\rho_{mm} - ig_1\rho_{Ym} + i\Omega_p\rho_{uu} - (\gamma_1 + \frac{3\gamma_d}{2})\rho_{um}, \quad (10)(11)$$

$$\dot{\rho}_{uY} = -i\Delta_1\rho_{uY} - i\Omega_p\rho_{mY} - ig_1\rho_{YY} + ig_1\rho_{uu} + ig_2\sqrt{2}\rho_{uG'} - (\gamma_1 + \frac{\kappa+\gamma_2+3\gamma_d}{2})\rho_{um}, \quad (12)$$

$$\dot{\rho}_{YG'} = -i\Delta_2\rho_{YG'} - ig_1\rho_{uG'} - ig_2\sqrt{2}\rho_{G'G'} + ig_2\sqrt{2}\rho_{YY} - (\frac{3\kappa+\gamma_2+\gamma_d}{2})\rho_{YG'}, \quad (13)$$

$$\dot{\rho}_{mY} = -i(\Delta_1-\Delta_p)\rho_{mY} - i\Omega_p^*(t)\rho_{uY} + ig_1\rho_{mu} + ig_2\sqrt{2}\rho_{mG'} - (\gamma_d + \frac{\kappa+\gamma_2}{2})\rho_{mY}, \quad (14)$$

$$\dot{\rho}_{uG'} = -i(\Delta_1+\Delta_2)\rho_{uG'} - i\Omega_p(t)\rho_{mG'} - ig_1\rho_{YG'} + ig_2\sqrt{2}\rho_{uY} - (\gamma_d+\kappa+\gamma_2)\rho_{uG'}, \quad (15)$$

$$\dot{\rho}_{mG'} = -i(\Delta_1+\Delta_2-\Delta_p)\rho_{mG'} - i\Omega_p^*(t)\rho_{uG'} + ig_2\sqrt{2}\rho_{mY} - (\kappa + \frac{\gamma_d}{2})\rho_{mG'}, \quad (16)$$

$$\dot{\rho}_{yG} = -i\Delta_2\rho_{yG} - ig_2\rho_{GG} + ig_2\rho_{yy} - \frac{(\kappa+\gamma_2+\gamma_d)}{2}\rho_{yG}, \quad (17)$$

When the pump field and the cavity mode satisfy the two-photon Raman resonance condition $\Delta_p \approx \Delta_1 + \Delta_2$, the evolution of the population in the QD energy levels follows the cavity-assisted STIRAP. Here, one must also remember that the Stark shifts of energy levels also play an important role in two-photon Raman resonance condition[16]. However, for constant cavity couplings, the Stark shifts in energy states remains constant and the two-photon Raman resonance condition can be satisfied easily by changing the detuning of the pump field (Δ_p) only.

In Fig. 2, we show the numerical simulations after solving Eqns. (3)-(17). The pump field is chosen to be a coherent superposition of two time-separated Gaussian pulses of the same width, but different amplitudes, which can be generated by passing a Gaussian pulse through an unbalanced two arm interferometer. The Rabi frequency of the pump field is given by $\Omega_p(t) = \Omega_1(t) + \Omega_2(t-T)$, where $\Omega_{1,2}(t)$ is the Rabi frequency of each pulse and T is the time gap between the pulses. We select a typical value of $\Omega_1(t)$ such that the population of the state $|m\rangle$ is pumped to the state $|y,1\rangle$ in STIRAP with probability

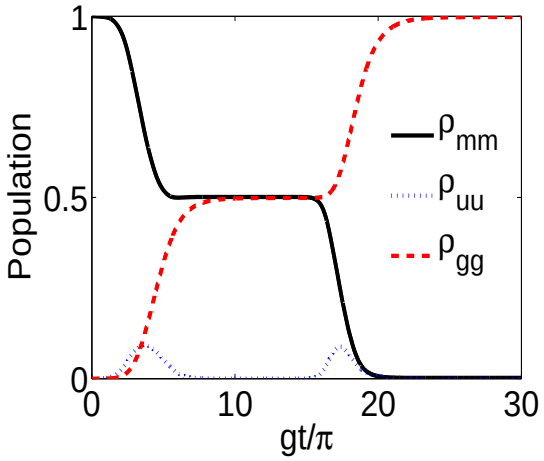

FIG. 2: (Color online)Populations in state $|m\rangle$ (black solid line), in state $|g\rangle$ (red dashed line) and in state $|u\rangle$ (blue dotted line) during the evolution. Two Gaussian pump pulses of different amplitude are employed such that $p_1 = p_2 = 1/2$. Using the parameters $g_1 = g_2 = g$, $\kappa = 2.5g$, $\gamma_2 = \gamma_1 = 10^{-3}g$, $\gamma_d = 10^{-2}g$, $\Delta_1 = -3g$, $\Delta_2 = 2g$, $\Delta_p = -1.5g$, $\Omega_1(t)/g = 0.74\exp[-(t-2\tau_p)^2/\tau_p^2]$, $\Omega_2(t)/g = 3\exp[-(t-9.5\tau_p)^2/\tau_p^2]$, and $g\tau_p = 2\pi$.

$p_1 = 1/2$. Due to the nature of the leaky cavity mode, the photon is emitted from the final state $|y,1\rangle$ and the system is evolved into the state $|y,0\rangle$ state. The population in state $|y,0\rangle$ is transferred to the state $|g,1\rangle$ through the cavity mode. After emitting another photon from the state $|g,1\rangle$, the system finally reaches the ground state $|g,0\rangle$. Thus a photon pair in the early time bin is emitted during the interaction of the first pulse $\Omega_1(t)$. The remaining population in state $|m\rangle$ is similarly pumped by another pulse $\Omega_2(t-T)$ and a photon pair is generated with probability $p_2 = 1-p_1$ in the late time bin. The state of the generated photon pair is thus maximally time-bin entangled state. For a QD embedded in a microcavity, the off-resonant exciton has a spontaneous decay rate of the order of $0.1-1\,\mu$eV ($10^{-3}g$ for $g = 0.1$ meV), and the cavity decay condition $\kappa >> g$ can be achieved easily. We stress that all of these parameters correspond closely to those in present day experiments[17,18].

During the time interaction with the pump pulses, the population in the upper state $|u\rangle$ remains always less that 0.1 and the population in $|g,2\rangle$ remains negligible. The state of emitted photon pair from the cavity mode can therefore be written as

$$|\psi(t)\rangle = \left[a_1^\dagger(t)a_2^\dagger(t) + a_1^\dagger(t-T)a_2^\dagger(t-T)\right]|\{0\}\rangle, \quad (18)$$

where $|\{0\}\rangle$ is vacuum field, $\langle a_1(t)\rangle = \langle\sigma_{yY}(t)\rangle$, and $\langle a_2(t)\rangle = \langle\sigma_{gG}(t)\rangle$, for $\sigma_{ij} = |i\rangle\langle j|$. In quantum information protocols, such as entanglement swapping, it is essential that the photons in the mode a_1 and a_2 should not have any other correlation except the time-bin entanglement. However, in the biexciton-exciton cascade, the a_1 mode photon is always generated after the emission of the a_2 mode photon. Thus the a_1 and a_2 modes

remain time correlated. This undesirable temporal correlation becomes negligible for $\Gamma_1/\Gamma_2 >> 1$[15], where Γ_i is the emission rate of the photon in a_i mode. In our scheme above, the first photon in mode a_1 is generated in resonant Raman process, which is emitted with the cavity mode decay rate κ, and the second photon is generated through cavity enhanced spontaneous emission. The condition $\Gamma_1/\Gamma_2 >> 1$ can therefore be easily satisfied by choosing a suitably large value of the detuning Δ_2 such that $g_2^2\kappa/(\kappa^2+\Delta_2^2) << \kappa$.

III. TRIPLE COINCIDENT DETECTION OF THE PHOTON ENTANGLEMENT, AND THE INFLUENCE OF PURE DEPHASING

Next, we discuss how to measure the entanglement of the generated state of the photons. The Concurrence of the state (18) is directly related to the coherence of the state[12]. For measuring the degree of entanglement, photons from each mode are passed through an unbalanced two path interferometer[5]; the time difference between two arms is T, with phase difference ϕ, and T is similar to the time difference between the two pulses in the pump fields. After passing through the interferometers, the field operators at the output of the interferometers can be expressed as

$$a_3(t) = a_1(t) + e^{i\phi}a_1(t-T), \tag{19}$$
$$a_4(t) = a_2(t) + e^{i\phi}a_2(t-T). \tag{20}$$

The post-selection, for detecting both photon simultaneously after passing through the interferometers, projects the state (18) into the state

$$|\psi_c(t)\rangle = \Big[a_1^\dagger(t)a_2^\dagger(t) + (1+e^{2i\phi})a_1^\dagger(t-T)a_2^\dagger(t-T) + a_1^\dagger(t-2T)a_2^\dagger(t-2T)\Big]|\{0\}\rangle. \tag{21}$$

Clearly, the state (21) has three terms which are distinguishable in time. The middle term, appearing at $t=T$, provides the information about the entanglement of state (18). For separating different terms in state (21), the time of detection of photons is measured with reference to the pump photons using a triple coincidence detection. The probability of triple coincidence detection of one photon at the output of each interferometer, and one from the input pulse Ω_1, is given by

$$G^{(3)}(\tau) = \int_0^\infty dt' \int_{-T_{bin}}^{T_{bin}} d\tau' |\Omega_1(t')|^2 \times \langle a_3^\dagger(t'+\tau)a_4^\dagger(t'+\tau+\tau')a_4(t'+\tau+\tau')a_3(t'+\tau)\rangle, \tag{22}$$

where T_{bin} is the width of the time-bins; which is chosen larger than the biexciton-exciton cascade decay and smaller than T. We can simplify the above expression for $G^{(3)}(\tau)$ using the property of field operators, $a_1(t)a_2(t-T)|\{0\}\rangle = 0$, as both photons are generated almost together in the cascade decay. Subsequently, we can simplify the correlation function in (22) as

$$\begin{aligned}\langle a_3^\dagger(t'+\tau)a_4^\dagger(t'+\tau+\tau')a_4(t'+\tau+\tau')a_3(t'+\tau)\rangle &= \langle a_1^\dagger(t'+\tau)a_2^\dagger(t'+\tau+\tau')a_2(t'+\tau+\tau')a_1(t'+\tau)\rangle \\ &+ \langle a_1^\dagger(t'-T+\tau)a_2^\dagger(t'-T+\tau+\tau')a_2(t'-T+\tau+\tau')a_1(t'-T+\tau)\rangle \\ &+ 2\cos 2\phi\langle a_1^\dagger(t'+\tau)a_2^\dagger(t'+\tau+\tau')a_2(t'-T+\tau+\tau')a_1(t'-T+\tau)\rangle, \end{aligned} \tag{23}$$

which is evaluated for state (18) by applying quantum regression formula[25]. We relegate the details of the $G^{(3)}$ calculation to the Appendix.

In Fig. 3, we plot $G^{(3)}(\tau)$ for the same parameters used in Fig. 2, where the time-dependent populations were shown. The computed value of $G^{(3)}(\tau)$ has three peaks centered at $\tau = 0$, T, and $2T$. The first peak at $\tau = 0$ correspond to the photons generated in the early time-bin that have passed through the short arms of the interferometers. Similarly the peak centered at $\tau = 2T$ corresponds to the photon pair generated in the late time-bin that have passed through the long arms of the interferometers. The central peak at $\tau = T$ corresponds to the overlap of the photons generated in early time bin and passed through the longer arms in the interferometers and the photons generated in the late time-bin and passed through the short arms. Thus only the central peak contains the information about the entanglement and can be easily selected by choosing a narrow time window around $\tau = T$. We have also found that the required value of T is slightly less than the actual time between the pump pulses, which shows that in STIRAP, the photons are actually generated before the pump pulse reaches its maximum. For the parameters used in Fig. 2, the time between pump pulses is $15\pi/g$, but the central peak in Fig. 3 is a maximum for $T = 14\pi/g$.

The coherence in the generated state (18) can be measured by varying the phase ϕ between the overlapping amplitudes corresponding to the early and the late time bins along the central peak. In Fig.4, we plot the interference pattern produced in the measurement of $P_c = \int_{T-T_{bin}}^{T+T_{bin}} G^{(3)}(\tau)d\tau$. The visibility of the interference pattern, defined as V=(maximum of P_c - minimum of P_c)/ (maximum of P_c + minimum of P_c), gives the

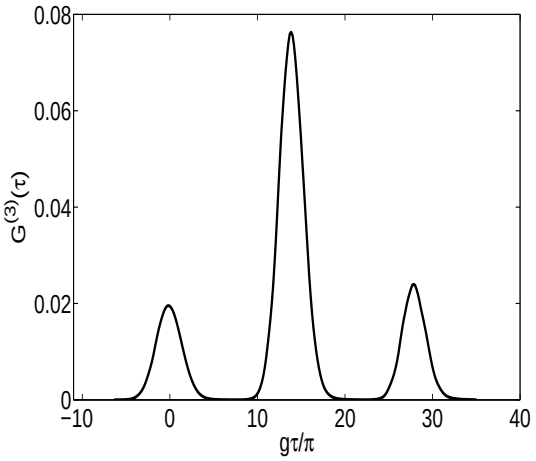

FIG. 3: The triple coincidence correlation of detecting one photon at output of each interferometer and one from the input pulse Ω_1 for $T = 14\pi/g$. The other parameters are the same as in Fig. 2

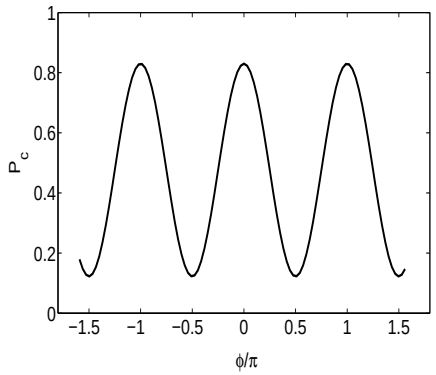

FIG. 4: The integrated value of the triple coincidence correlation $G^{(3)}(\tau)$ along the central peak at $\tau = T$. The interference pattern appears on changing the phase ϕ produced by the interferometers.

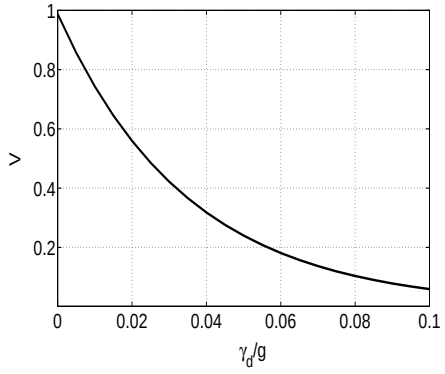

FIG. 5: The dependence of the visibility, i.e. entanglement of the generated time-bin entangled state of the photon on dephasing rate γ_d.

concurrence and the purity of the generated state (18).

In Fig. 5, we show the dependence of the visibility on the dephasing rate. In the presence of pure dephasing, the visibility, i.e. concurrence of the generated state (Eq. 18), is strongly inhibited. Further the dephasing in the state (Eq. 18) only occurs during the interaction of the pump pulses. The dephasing during the time gap between the pump pulses plays no role as the coherence in the state is produced by the coherence between the input pulses. The inhibition of interference due to dephasing can be understood as due to pure dephasing (e.g., phonon) interactions the information about the photon generating in different time bin is partially imprinted in the phonon baths and thus as a result of quantum complementarity the interference is inhibited. However, for small dephasing rate $\gamma_d \approx 0.01 g_1$, the value of visibility is larger than $1/\sqrt{2}$, which is required for violation of Bell's inequalities[26].

IV. CONCLUSIONS

We have presented a cavity-QED STIRAP scheme for generating a scalable source of time-bin entangled photon pairs, and we also investigated the role of pure dephasing on entanglement. The generated state of the photons can be detected by measuring the correlations between the pump and the generated photons. We found that for small values of pure dephasings, it is possible to achieve larger values of entanglement using current working technologies.

V. ACKNOWLEDGEMENTS

This work was supported by the National Sciences and Engineering Research Council of Canada, and the Canadian Foundation for Innovation. We acknowledge useful discussions with Robin Williams and Gregor Weihs.

Appendix: Calculation of multi-time correlations

Here we briefly discuss the method for calculating two-time correlation and four-time correlation used in Sec. III. We follow the approach discussed by Gardiner and Zoller[25] for evaluating multi-time correlations. The required two time correlation can be expressed as

$$\begin{aligned}
&\langle a_1^\dagger(t) a_2^\dagger(t+\tau) a_2(t+\tau) a_1(t)\rangle \\
&= Tr\left\{a_2(t+\tau) a_1(t)\rho(0) a_1^\dagger(t) a_2^\dagger(t+\tau)\right\} \quad \text{(A.1)} \\
&= Tr\left\{a_2(t+\tau)\rho'(t) a_2^\dagger(t+\tau)\right\}, \quad \text{(A.2)} \\
&= Tr\left\{a_2\rho'(t+\tau) a_2^\dagger\right\} \quad \text{(A.3)}
\end{aligned}$$

where Tr stands for trace and operators a_i appearing without time parenthesis are in Schrodinger picture,

$\rho'(t) = a_1(t)\rho(0)a_1^\dagger(t) = a_1\rho(t)a_1^\dagger$ is calculated after evolving the initial state $\rho(0) = \rho_{mm}|m\rangle\langle m|$ for time t using Eqs.(3)-(17) and then operating by a_1 and $a_1^\dagger$ from left and right, respectively. Clearly, ρ' also follows the same equations of motions (3)-(17). Now, using initial value $\rho'(t) = a_1\rho(t)a_1^\dagger$ at time t, and evolving for time τ, $\rho'(t+\tau)$ is calculated. The value of the required correlation is calculated using Eq. (A.3). A similar straightforward approach, considering the times appearing in the a operators in ascending order, is applied in evaluating the four time correlations as follows:

$$\begin{aligned}
&\langle a_1^\dagger(t)a_2^\dagger(t+\tau)a_2(t-T+\tau)a_1(t-T)\rangle,\\
&= Tr\left\{a_2(t-T+\tau)a_1(t-T)\rho(0)a_1^\dagger(t)a_2^\dagger(t+\tau)\right\} && \text{(A.4)}\\
&= Tr\left\{a_2(t-T+\tau)\rho_1(t-T)a_1^\dagger(t)a_2^\dagger(t+\tau)\right\}, && \text{(A.5)}\\
&= Tr\left\{\rho_2(t-T+\tau)a_1^\dagger(t)a_2^\dagger(t+\tau)\right\}, && \text{(A.6)}\\
&= Tr\left\{\rho_3(t)a_2^\dagger(t+\tau)\right\}, && \text{(A.7)}\\
&= Tr\left\{\rho_3(t+\tau)a_2^\dagger\right\}, && \text{(A.8)}
\end{aligned}$$

where $\rho(0) = \rho_{mm}|m\rangle\langle m|$, $\rho_1(t-T) \equiv a_1(t-T)\rho(0) \equiv a_1\rho(t-T)$, $\rho_2(t-T+\tau) \equiv a_2(t-T+\tau)\rho_1(t-T) \equiv a_2\rho_1(t-T+\tau)$, and $\rho_3(t) \equiv \rho_2(t-T+\tau)a_1^\dagger(t) \equiv \rho_2(t)a_1^\dagger$. Thus the density matrices ρ, ρ_1, ρ_2, and ρ_3 are evolved for times, 0 to $t-T$, $t-T$ to $t-T+\tau$, $t-T+\tau$ to t, and t to $t+\tau$ respectively. The evolution of $\rho(0)$ is given by Eqs. (3)-(17), while the evolutions of density matrices ρ_i for i=1,2,3, follow the similar equations, written for ρ, as

$$\begin{aligned}
\dot\rho_{Yy} &= -ig_1\rho_{uy} - ig_2\sqrt{2}\rho_{G'y} + ig_2\rho_{YG}\\
&\quad -(\gamma_2+\kappa/2+\gamma_d)\rho_{Yy}, && \text{(A.9)}\\
\dot\rho_{G'G} &= -ig_2\sqrt{2}\rho_{YG} + ig_2\rho_{G'y} - \frac{3}{2}\kappa\rho_{G'G}, && \text{(A.10)}\\
\dot\rho_{Gg} &= -ig_2\rho_{yg} - \frac{1}{2}\kappa\rho_{Gg}, && \text{(A.11)}\\
\dot\rho_{uy} &= -i\Delta_1\rho_{uy} - i\Omega_p(t)\rho_{my} - ig_1\rho_{Yy} + ig_2\rho_{uG}\\
&\quad -(\gamma_1+\gamma_2/2+3\gamma_d/2)\rho_{uy}, && \text{(A.12)}\\
\dot\rho_{G'y} &= i\Delta_2\rho_{G'y} - ig_2\sqrt{2}\rho_{Yy} + ig_2\rho_{G'G}\\
&\quad -(\kappa+\gamma_2/2+\gamma_d/2)\rho_{G'y}, && \text{(A.13)}\\
\dot\rho_{YG} &= -i\Delta_2\rho_{YG} - ig_1\rho_{uG} - ig_2\sqrt{2}\rho_{G'G} + ig_2\rho_{Yy}\\
&\quad -(\kappa+\gamma_2/2+\gamma_d/2)\rho_{YG}, && \text{(A.14)}\\
\dot\rho_{yg} &= -i\Delta_2\rho_{yg} - ig_2\rho_{Gg} - \frac{1}{2}(\gamma_2+\gamma_d)\rho_{yg}, && \text{(A.15)}\\
\dot\rho_{my} &= -i(\Delta_1-\Delta_p)\rho_{my} - i\Omega_p^*(t)\rho_{uy} + ig_2\rho_{mG}\\
&\quad -(\gamma_2/2+\gamma_d)\rho_{my}, && \text{(A.16)}\\
\dot\rho_{uG} &= -i(\Delta_1+\Delta_2)\rho_{uG} - i\Omega_p\rho_{mG} - ig_1\rho_{YG} + ig_2\rho_{uy}\\
&\quad -(\kappa/2+\gamma_1+\gamma_d)\rho_{uG}, && \text{(A.17)}\\
\dot\rho_{mG} &= -i(\Delta_1+\Delta_2-\Delta_p)\rho_{mG} - i\Omega_p^*(t)\rho_{uG} + ig_2\rho_{my}\\
&\quad -\frac{1}{2}(\kappa+\gamma_d)\rho_{mG}, && \text{(A.18)}\\
\dot\rho_{G'g} &= -ig_2\sqrt{2}\rho_{Yg} - \kappa\rho_{G'g}, && \text{(A.19)}\\
\dot\rho_{Yg} &= -i\Delta_2\rho_{Yg} - ig_2\sqrt{2}\rho_{G'g} - ig_1\rho_{ug}\\
&\quad -\frac{1}{2}(\kappa+\gamma_2+\gamma_d)\rho_{Yg}, && \text{(A.20)}\\
\dot\rho_{ug} &= -i(\Delta_1+\Delta_2)\rho_{ug} - i\Omega_p\rho_{mg} - ig_1\rho_{Yg}\\
&\quad -(\gamma_1+\gamma_d)\rho_{ug}. && \text{(A.21)}
\end{aligned}$$

Finally, the value of four-times correlations used in Sec.III are found using Eq. (A.8).

[1] W. Tittel, and G. Weihs, Quant. Inform. Comput. **1**, 3 (2001); M. A. Nielsen, and I. L. Chuang, Quantum Computation and Quantum Information (Cambridge Univ. Press, Cambridge, 2000).

[2] A. K. Ekert, Phys. Rev. Lett. **67**, 661 (1991); T. Jennewein, C. Simon, G. Weihs, H. Weinfurter, and A. Zeilinger, Phys. Rev. Lett. **84**, 4729 (2000); D. S. Naik, C. G. Peterson, A. G. White, A. J. Berglund, and P. G. Kwiat, *ibid.* **84**, 4733 (2000).

[3] C. H. Bennett, G. Brassard, C. Crpeau, R. Jozsa, A. Peres, and W. K. Wootters, Phys. Rev. Lett. **70**, 1895 (1993); D. Bouwmeester, J.-W. Pan, K. Mattle, M. Eibl, H. Weinfurter, A. Zeilinger, Nature (London) **390**, 575 (1997); D. Boschi, S. Branca, F. De Martini, L. Hardy, and S. Popescu, Phys. Rev. Lett. **80**, 1121 (1998).

[4] P. G. Kwiat, K. Mattle, H. Weinfurter, A. Zeilinger, A. V. Sergienko, and Y. Shih, Phys. Rev. Lett. **75**, 4337 (1995).

[5] W. Tittel, J. Brendel, H. Zbinden, and N. Gisin, Phys. Rev. lett **81**, 3563 (1998).

[6] J. Brendel, N. Gisin, W. Tittel, and H. Zbinden, Phys. Rev. Lett. **82**, 2594 (1999); W. Tittel, J. Brendel, H. Zbinden, and N. Gisin Phys. Rev. Lett. **84**, 4737 (2000).

[7] I. Marcikic, H. de Riedmatten, W. Tittel, V. Scarani, H. Zbinden, and N. Gisin, Phys. Rev. A **66**, 062308 (2002).

[8] I. Marcikic, H. de Riedmatten, W. Tittel, H. Zbinden, M. Legr, and N. Gisin, Phys. Rev. Lett. **93**, 180502 (2004).

[9] L. Mandel and E. Wolf, *Optical Coherence and Quantum Optics* (Cambridge University Press, Cambridge, England, 1995).

[10] P. Zoller, Th. Beth, D. Binosi, R. Blatt, H. J. Briegel, D. Bruss, T. Calarco, J. I. Cirac, D. Deutsch, J. Eisert, A. Ekert, C. Fabre, N. Gisin, P. Grangiere, M. Grassl, S. Haroche, A. Imamoglu, A. Karlson, J. Kempe, L. Kouwenhoven, S. Krll, G. Leuchs, M. Lewenstein, D. Loss, N. Ltkenhaus, S. Massar, J.E. Mooij, M. B. Plenio, E. S. Polzik, S. Popescu, G. Rempe, A. Sergienko, D. Suter, J. Twamley, G. Wendin, R. Werner, A. Winter, J. Wrachtrup, A. Zeilinger, Eur. Phys. J. D 36/2, 203 (2005).

[11] C. Santori, D. Fattal, J. Vuckovic, G. S. Solomon, Y. Yamamoto, Nature **419**, 594 (2002); D. Fattal, K. Inoue, J. Vuckovic, C. Santori, G. S. Solomon, and Y. Yamamoto, Phys. Rev. Lett. **92**, 037903 (2004); R. B. Patel, A. J. Bennett, K. Cooper, P. Atkinson, C. A. Nicoll, D. A. Ritchie, and A. J. Shields, Phys. Rev. Lett. **100**, 207405 (2008).

[12] N. Akopian, N. H. Lindner, E. Poem, Y. Berlatzky, J. Avron, D. Gershoni, B. D. Gerardot, and P. M. Petroff, Phys. Rev. lett **96**, 130501 (2006).

[13] R. M. Stevenson, R. J. Young, P. Atkinson, K. Cooper, D. A. Ritchie, and A. J. Shields, Nature (London) **439**, 179 (2006); R. M. Stevenson, R. J. Young, P. See, D. G. Gevaux, K. Cooper, P. Atkinson, I. Farrer, D. A. Ritchie, and A. J. Shields, Phys. Rev. B **73**, 033306 (2006); K. Kowalik, O. Krebs, A. Golnik, J. Suffczyn'ski, P. Wojnar, J. Kossut, J. A. Gaj, and P. Voisin, Phys. Rev. B **75**, 195340 (2007).

[14] B. D. Gerardot, S. Seidl, P. A. Daigarno, R. J. Warburton, D. Granados, J. M. Garcia, K. Kowalik, and O. Krebs, Appl. Phys. Lett. **90**, 041101 (2007); M. M. Vogel, S. M. Ulrich, R. Hafenbrak, P. Michler, L. Wang, A. Rastelli, and O. G. Schmidt, Appl. Phys. Lett. **91**, 051904 (2007).

[15] C. Simon and J. Poizat, Phys. Rev. Lett. **94**, 030502 (2005).

[16] L. P. Yatsenko, S. Gurin, T. Halfmann, K. Bhmer, B. W. Shore, and K. Bergmann, Phys. Rev. A **58**, 4683 (1998); S. Gurin, L. P. Yatsenko, T. Halfmann, B. W. Shore, and K. Bergmann, Phys. Rev. A **58**, 4691 (1998).

[17] E. B. Flagg, A. Muller, J. W. Robertson, S. Founta, D. G. Deppe, M. Xiao, W. Ma, G. J. Salamo, and C. K. Shih, Nature Phys. **5**, 203 (2009); E. B. Flagg, A. Muller, S. V. Polyakov, A.Ling, A. Migdall, and G. S. Solomon, Phys. Rev. Lett. **104**, 137401 (2010).

[18] S. Ates, S. M. Ulrich, S. Reitzenstein, A. Lffler, A. Forchel, and P. Michler, Phys. Rev. Lett. **103**, 167402 (2009); S. Ates, S. M. Ulrich, A. Ulhaq, S. Reitzenstein, A. Lffler, S. Hfling, A. Forchel, and P. Michler, Nature Photonics **3**, 724 (2009).

[19] A. Faraon, A. Majumdar, H. Kim, P. Petroff, and J. Vuckovic, Phys. Rev. Lett. **104**, 047402 (2010).

[20] V. Stavarache et al., Appl. Phys. Lett. **89**, 123105 (2006); X. Xu et al., New J. Phys. **10**, 053036 (2008); W. Heller et al., Phys. Rev. B **57**, 6270 (1998).

[21] P. K. Pathak and S. Hughes, Phys. Rev. B **80**, 155325 (2009).

[22] M. E. Reimer et al., Phys. Rev. B **78**, 195301 (2008).

[23] S. Rodt, R. Heitz, A. Schliwa, R. L. Sellin, F. Guffarth, and D. Bimberg, Phys. Rev. B 68, 035331 (2003).

[24] F. Ding, R. Singh, J. D. Plumhof, T. Zander, V. Krapek, Y. H. Chen, M. Benyoucef, V. Zwiller, K. Dorr, G. Bester, A. Rastelli, and O. G. Schmidt Phys. Rev. Lett. **104**, 067405 (2010).

[25] C. W. Gardiner, P. Zoller, *Quantum Noise, A Handbook of Markovian and Non-Markovian Quantum Stochastic Methods with Applications to Quantum Optics* (Springer, Berlin 2004).

[26] F. Verstraete and M. M. Wolf, Phys. Rev. Lett., **89**, 170401 (2002).